Crystal Structure of the Sensor Domain of the BlaR Penicillin Receptor from *Bacillus licheniformis*[†,‡]

Frédéric Kerff,[§,||] Paulette Charlier,[§] Maria-Luigi Colombo,[⊥] Eric Sauvage,[§] Alain Brans,[⊥] Jean-Marie Frère,[⊥] Bernard Joris,[⊥] and Eveline Fonzé*[,§]

Institut de Physique B5 and Institut de Chimie B6, Centre d'Ingénierie des Protéines, Université de Liège, B-4000 Sart Tilman, Belgium

Received June 6, 2003; Revised Manuscript Received August 26, 2003

ABSTRACT: As in several staphylococci, the synthesis of the *Bacillus licheniformis* 749/I β-lactamase is an inducible phenomenon regulated by a signal-transducing membrane protein BlaR. The C-terminal domain of this multimodular protein is an extracellular domain which specifically recognizes β-lactam antibiotics. When it binds a β-lactam, a signal is transmitted by the transmembrane region to the intracellular loops. In response, the hydrolytic activity of the BlaR large cytoplasmic L3 loop is induced, and a cascade of reactions is generated, leading to the transcription of the β-lactamase gene. Here, we describe the crystal structure of the extracellular penicillin-receptor domain of BlaR (residues 346−601) at 2.5 Å resolution in order to understand why this domain, whose folding is very similar to that of class D β-lactamases, behaves as a highly sensitive penicillin-binding protein rather than a β-lactamase. Two residues of the BlaR C-terminal domain, Thr452 and Thr542, modify the hydrophobic characteristic of the class D β-lactamase active site. Both residues seem to be in part responsible for the lack of β-lactamase activity of the BlaR protein due to the stability of the acyl-enzyme. Although further experimental data are needed to fully understand the transmembrane induction process, the comparison of the BlaR sensor domain structure with those of class D β-lactamase complexes and penicillin-binding proteins provides interesting elements to hypothesize on possible signal transmission mechanisms.

The most common resistance system developed by bacteria against β-lactam antibiotics is the production of hydrolytic enzymes that degrade the antibiotics into inactive metabolites. The production of these β-lactamases can be regulated by a signal-transducing integral membrane protein, BlaR, and a transcriptional repressor, BlaI. This regulating pathway has been described in *Bacillus licheniformis* (*1*, *2*) and several staphylococci (*3*). Another related pathway mediates resistance to β-lactam antibiotics and has been described in staphylococci. It involves the production of PBP2a, a low-affinity penicillin-binding transpeptidase that can substitute for other penicillin-binding proteins (PBPs),[1] allowing further peptidoglycan synthesis. The synthesis of PBP2a is regulated in the same way as β-lactamase production, involving a similar sensor−transducer, MecR1, and the MecI repressor. The signal transducers BlaR and MecR are multimodular proteins with penicillin-binding domains that specifically recognize β-lactam antibiotics outside the cell and then transmit a signal to the cytoplasm that derepresses the transcription of the β-lactamase and PBP2a genes. The BlaR and MecR proteins share a high degree of homology, and the sequences of their penicillin-binding domains are closer to those of class D β-lactamases than to any other PBPs (*4*).

In *B. licheniformis* 749/I, the sensor−transducer BlaR is a 601 residue protein (Figure 1). Its N-terminal domain (BlaR-NTD, residues 1−345) begins with a short extracellular segment (eight amino acids) and is anchored into the membrane by four transmembrane segments (TM1, TM2, TM3, and TM4) interconnected by three loops (L1, L2, and L3). The large cytoplasmic loop L3 (residues 137−320) connects the transmembrane segments TM3 and TM4 and contains a His212-Glu-Xaa-Xaa-His sequence, a zinc-binding motif characteristic of the metalloproteases belonging to the thermolysin family. It is very probably a zinc hydrolase (*2*). The extracellular penicillin sensor domain of BlaR is located at the end of the polypeptide chain (residues 346−601) of the penicillin receptor and is hereafter referred to the BlaR C-terminal domain (BlaR-CTD).

When an inducing β-lactam antibiotic is present in the external environment, the penicillin sensor, BlaR-CTD, is acylated and generates a transmembrane signal that activates

[†] This work was supported in part by the Belgian Program on Interuniversity Poles of Attraction initiated by the Belgian State, Prime Minister's Office, Science Policy Programming (PAI P5/33), by the Fonds National de la Recherche Scientifique (FNRS, credit aux chercheurs 1.5201.02, FRFC 2.4530.03, and IISN 4.4505.00), and by a contract between the Région Wallonne and the University of Liège (convention 981/3699). B.J. is Research Associate of the FNRS.

[‡] Atomic coordinates have been deposited in the Protein Data Bank (code 1nrf) at Rutgers University.

* Corresponding author: phone, 32.43.66.36.19; fax, 32.43.66.36.67; e-mail, eveline.fonze@ulg.ac.be.

[§] Institut de Physique B5, The University of Liege.

[||] Present address: Boston Biomedical Research Institute, 64 Grove St., Watertown, MA 02472.

[⊥] Institut de Chimie B6, The University of Liege.

[1] Abbreviations: PBPs, penicillin-binding proteins; BlaR-NTD, BlaR N-terminal domain; BlaR-CTD, BlaR C-terminal domain; PDB, Protein Data Bank; rms, root mean square.

10.1021/bi034976a CCC: $25.00
Published on Web 10/16/2003

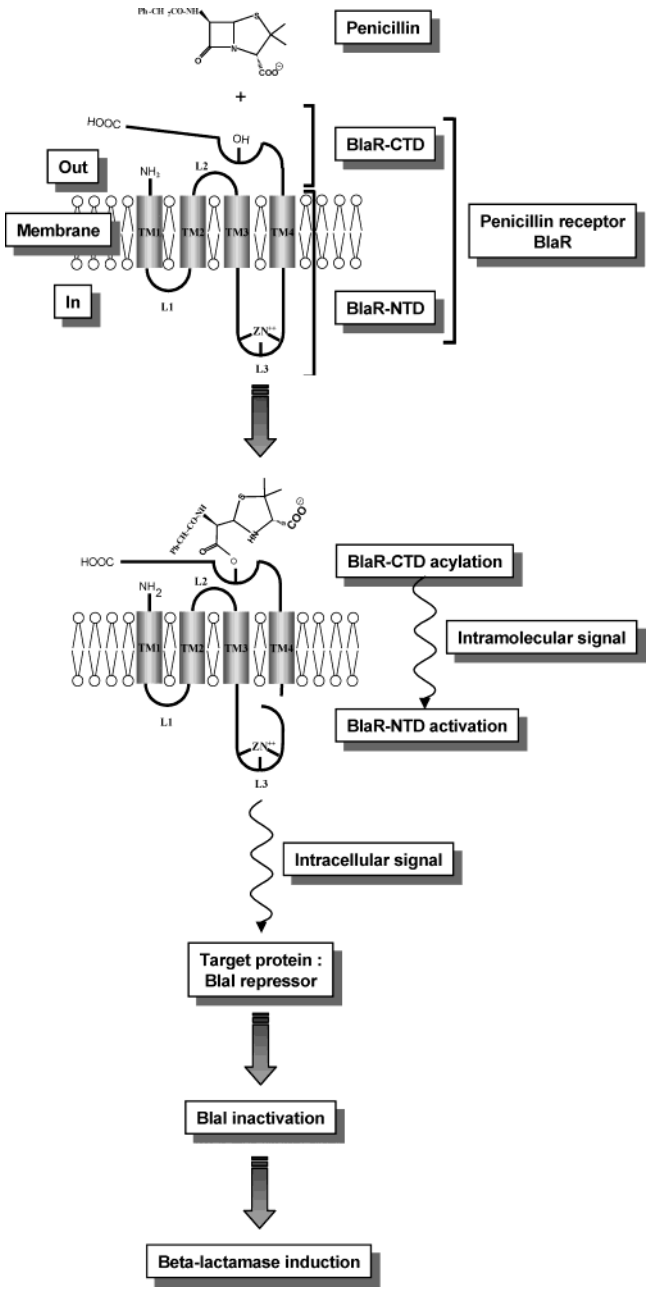

FIGURE 1: Schematic representation of BlaR signal transduction. BlaR-NTD and BlaR-CTD are abbreviations for BlaR N-terminal (residues 1−345) and BlaR C-terminal (residues 346−601) domains. TM1, TM2, TM3, and TM4 are the four transmembrane segments, and L1, L2, and L3 are the three loops of the penicillin receptor. In BlaR-CTD, −OH represents the active site serine which is acylated by β-lactam.

the hydrolytic activity of the L3 loop. The target of the signal launched by L3 in the cytoplasm is the DNA-binding protein BlaI that controls the transcription of the β-lactamase *blaP* gene. In the absence of inducer, BlaI is bound to its DNA operator sequence and inhibits the transcription of the β-lactamase gene. In the presence of the inducer, the inactivation of BlaI allows RNA polymerase to access the *blaP* gene (*5*). The mechanism of β-lactamase induction reported in *Staphylococcus aureus* (*3*) varies only in the details. In *S. aureus*, it has been shown that hydrolysis of BlaI is the direct consequence of the acylation of BlaR by penicillin and is concomitant with the self-activation of the L3 hydrolase by cleavage of the peptide bond between Arg293 and Arg294. In *B. licheniformis*, acylation of the BlaR receptor by the inducer also results in activation of the L3 loop by self-proteolysis (Benlafya and Joris, unpublished results), but the BlaI repressor is inactivated by the binding of a coactivator. This coactivator would be generated by the hydrolytic action of the activated L3 loop on a procoactivator (*6*). Although the substrate of the L3 loop seems to be different in *S. aureus* and *B. licheniformis*, the first step in the induction process is in both cases the acylation of BlaR-CTD by penicillin.

The soluble forms of BlaR-CTD from *B. licheniformis* and *S. aureus*, respectively, overexpressed in the periplasm and cytoplasm of *Escherichia coli*, can be acylated by a wide variety of β-lactam antibiotics (*7*−*9*), and they both exhibit similar kinetic parameters. In the case of BlaR-CTD from *S. aureus*, it was reported that the catalytic activity of the penicillin sensor depends, as described for class D β-lactamases, on the modification of an active site lysine (Lys70) by carbonic anhydride to form a derivative of carbamic acid (*9*). The carbonation of this lysine is highly pH dependent and is only fully obtained at pH values greater than 8.0. In this paper, we report the crystallographic structure of the *B. licheniformis* BlaR-CTD at 2.5 Å resolution. Our structural analysis, supported by kinetic data, suggests that, by contrast with the class D β-lactamases, the corresponding active site lysine residue is not modified. By comparing this structure to those of PBPs and β-lactamases, one can tentatively explain how the acylation of the C-terminal domain results in signal genesis and transmission.

MATERIALS AND METHODS

Protein Production, Crystallization, and Data Collection. BlaR-CTD was cloned, expressed, and purified as described previously (*8*). Prior to the crystallization, the protein solution was concentrated to approximately 20 mg/mL by ultrafiltration using an Ultrafree-MC concentrator (Millipore) with a 5 kDa cutoff. The initial crystallization conditions were established using sparse matrix sampling (*10*) with the hanging drop vapor diffusion method (*11*) at 293 K using the different commercially available crystallization kits (Hampton Research, Emerald Biostructures). Drops were prepared by mixing 2 μL of protein solution to 2 μL of reservoir solution. Crystals of small size and poor quality could only be obtained in condition numbers 18 and 22 of the Crystalscreen formulations from Hampton Research. The crystallization conditions were further optimized by an extensive search around these conditions and by testing additives. Addition of chloride salts in the crystallization solution enhanced the size of the crystals and the reproducibility of crystal growth. The best crystals grew as cluster of needles (800 × 50 × 50 μm) from 18% PEG 8000, 5% glycerol, and 50 mM $CaCl_2$ in 0.1 M cacodylate buffer, pH 6.95.

Before the X-ray data collection, the BlaR-CTD crystal was flash frozen in liquid nitrogen after rapid soaking in a cryoprotectant solution containing 25−35% glycerol in the crystallization buffer. Data were collected at ESRF (European Synchrotron Radiation Facility, Grenoble, France) on beamline BM30A at a wavelength value of 0.9786 Å. All data were recorded on a MarCCD detector, and intensities were

Table 1: X-ray Data Collection and Refinement Statistics[a]

Diffraction Data[a]	
space group; cell parameters (Å)	$P4_1$; $a = b = 45.85$, $c = 130.198$
resolution (Å)	32.44−2.44 (2.50−2.44)
unique reflections; completeness (%)	9979 (745); 99.7 (99.9)
av $I/\sigma(I)$; R_{merge}[b] (%)	8.9 (3.7); 6.8 (23.2)
Refined Model	
resolution range (Å)	31.5−2.5
completeness (working + test) (%)	94.1
no. of reflections ($F > 2\sigma$)	8827
R[c] (working set)/R_{free} (test set) (%)	20.4/25.7
estd error of R_{free} value	0.012
protein/solvent atoms (non-H)	2005/81
B values from Wilson plot/ mean value (Å^2)	40.3/40.0
estd coordinate error from (low-resolution cutoff of 5.0 Å) Luzzati plot/sigma A (Å)	0.27/0.20
rmsd from ideal values	
bond lengths/bond angles (Å/deg)	0.007/1.1
dihedral angles/improper angles (deg)	23.1/0.74

[a] Data for highest resolution shell are in parentheses. [b] $R_{merge}(I) = \sum_{hlk}|I_{hkl} - \langle I_{hkl}\rangle|/\sum_{hlk}I_{hkl}$, where I_{hkl} is the measured intensity of the reflection with the indices hkl. [c] $R = \sum_{hlk}||F_{o,hkl}| - |F_{c,hkl}||/\sum_{hlk}F_{o,hkl}$, where $|F_{o,hkl}|$ and $|F_{c,hkl}|$ are the observed and calculated structure factor amplitudes for reflection hkl belonging to the working set. R_{free} is defined for reflection hkl belonging to the test set, which contains 5.1% of all reflections.

indexed and integrated using MOSFLM version 6.01 (*12*). This single crystal, belonging to space group $P4_1$ with unit cell dimensions $a = b = 45.85$ Å and $c = 130.20$ Å, diffracted to about 2.46 Å resolution. The scaling of the intensity data was accomplished with SCALA of the CCP4 program suite (*13*), and all corresponding statistics are given in Table 1.

Phasing Procedure and Structure Refinement. As various studies of the BlaR protein had indicated that its C-terminal domain presents high sequence similarity with class D β-lactamases, and particularly the OXA-2 β-lactamase from *Salmonella typhimurium* (PDB code 1K38) (*36*), the phasing procedure for solving the BlaR-CTD crystal structure was the molecular replacement method. The rotational and translational parameter investigations were performed with the AMORE package (*14*), using as search model the coordinates of only one monomer of the OXA-2 structure, with solvent molecules removed. To validate the molecular replacement solution, the same trials were performed using the coordinates of the *Pseudomonas aeruginosa* OXA-10 β-lactamase (PDB code 1K4F) (*36*). As the amino acid sequence identities were about 32% and 24% when BlaR-CTD is compared with OXA-2 and OXA-10, respectively, the first electron density maps were computed at 2.8 Å resolution. The model based on the OXA-2 structure was progressively modified by fitting to the electron density maps using TURBO-FRODO (*15*). The maps were of type $2F_o - F_c$ and $F_o - F_c$ weighted with sigma coefficients, as implemented in CNS (*16*), and the most ambiguous regions with unclear electron density were rebuilt on the basis of omit maps. Alternated cycles of refinement by simulated annealing using the maximum likehood method including a bulk solvent correction were performed with CNS. When the model could no longer be improved, 81 water molecules were added on the basis of the difference ($F_o - F_c$) electron density map. The BlaR-CTD structure was refined to 2.5 Å resolution, and the statistics of refinement are summarized in Table 1. Coordinates and structure factors have been deposited in the Protein Data Bank (http://www.rcsb.org; accession code 1NRF). Figures were prepared with MOLSCRIPT/RASTER3D (*17*).

Determination of Kinetic Parameters. The BlaR-CTD protein was dialyzed against a 50 mM sodium phosphate buffer, pH 8, containing 50 mM NaCl. The concentration of the protein was determined spectrophotometrically by measuring its absorbance at 280 nm ($A_{1cm}^{280nm} = 1.55$ for 1 mg/mL pure BlaR-CTD). The k_2/K rate constants were determined at room temperature with a UVIKON 940 (KONTRON instrument) spectrophotometer and a Copam + PC 88C microcomputer. The parameters for the reaction between BlaR-CTD and cefalexin were directly determined by monitoring the formation of the acyl-enzyme at 260 nm. This is accompanied by a decrease of the absorbance of the mixture due to the opening of the β-lactam ring ($\Delta\epsilon = -4850$ cm^{-1}·M^{-1}). The experiments were carried out in phosphate buffer degassed or not degassed and with addition of 50 mM bicarbonate. The observed rate constants were measured at a protein concentration of 15 μM and a cefalexin concentration of 50 μM. The reaction was monitored for 120 s, which yielded full acylation of the protein. To make sure that a pseudo-first-order rate constant was correctly measured, the k_a value was derived from the data recorded before more than 30% of the protein was acylated. Since the value of K was well above the cefalexin concentration (*8*), the value of k_2/K was directly derived from $k_a = (k_2/K)[I]$, where [I] was the cefalexin concentration.

RESULTS

Structure Determination. The 3D structure of the extracellular penicillin-receptor domain of BlaR (residues Gln346 to Arg601) has been determined by X-ray crystallography. The thin needle-shaped crystal diffracted to about 2.46 Å with a significant signal-to-noise ratio and corresponded to a tetragonal form with unit cell axes $a = b = 45.85$ Å and $c = 130.20$ Å (Table 1). With these dimensions and considering the molecular mass of the protein (26000 Da), the asymmetric unit could only contain one BlaR-CTD molecule, with about 46% of solvent content, and the space groups $P4$, $P4_1$, $P4_2$, and $P4_3$ were possible candidates. The general reflection conditions ($00l$:$l = 4n$) observed in the diffraction pattern corresponded to the $P4_1$ and $P4_3$ tetragonal forms. Using molecular replacement as the phasing method, the accurate space group was deduced on the basis of translational parameter investigations. With both class D β-lactamases, OXA-2 from *S. thyphimurium* and OXA-10 from *P. aeruginosa*, as search molecules, a clear translation solution appeared only in space group $P4_1$. The first model of BlaR-CTD was built in the $2F_o - F_c$ and $F_o - F_c$ electron density maps with phases computed from the OXA-2 atomic coordinates at 2.8 Å resolution. Mostly composed of all atoms of the buried core and of polyalanine chains for the more ambiguous regions, this first model exhibited R and R_{free} values of 31.6% and 41.8%, respectively. After some 15 alternated cycles of refinement/rebuilding, the BlaR-CTD structure was refined to 2.5 Å resolution with R and R_{free} values of 20.4% and 25.7%, respectively (Table 1).

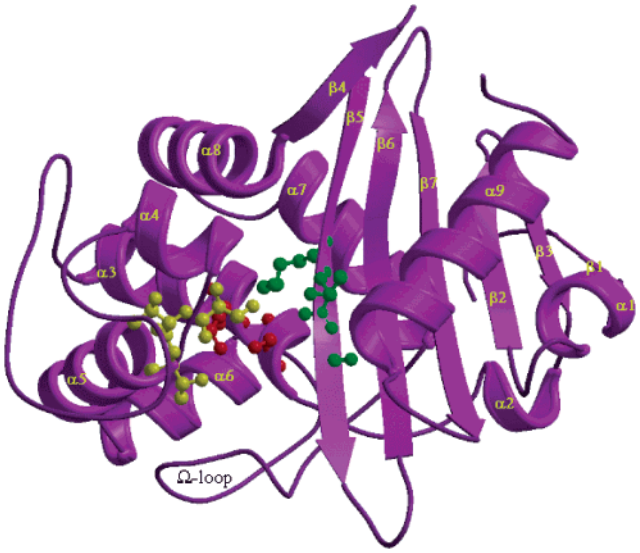

FIGURE 2: Ribbon diagram of the *B. licheniformis* BlaR penicillin-receptor domain with the identification of the conserved motifs of the active site. The Ser402-Thr-Tyr-Lys405 tetrad, including the nucleophilic serine of motif 1, is in red, the Ser450-Thr-Thr452 motif 2 is in yellow, and the Lys539-Thr-Gly541 triad of motif 3 is in green.

Overall Structure. The BlaR-CTD crystal structure consists of 246 amino acid residues defining the protein from Phe352 to Pro597 and 81 water molecules. The electron density around the N- and C-terminal regions was unclear, and the corresponding residues, Gln340 to Arg351 and Ser598 to Arg601, respectively, which are certainly disordered in the crystal, were not included in the structure. The polypeptide chain obviously exhibits the typical fold of class D β-lactamases, organized into two domains with the catalytic pocket at their interfaces (Figure 2). One domain of α/β type consists of a seven-stranded antiparallel β-sheet (β1 to β7) covered on one face by two α-helices (α1 and the C-terminal α9) and on the other face by a one-turn helix α2 and helix α7. The second domain, mainly all-α, contains a hydrophobic central helix (α3) surrounded by four helices (α4 to α6 and α8). More precisely, the α3 helix corresponds to one turn of a 3_{10} helix followed by four turns of an α-type helix.

All of these secondary structure elements are connected by various loops. The two largest ones are the α3−α4 interconnecting loop and the Ω-loop (so-called by analogy with class A β-lactamases) between α6 and α7, which are respectively 27 and 23 amino acid residues long. The α3−α4 loop (Gly416−Asp442) can be considered as a "mobile loop". Being on the surface of the molecule, it makes very few interactions with the protein core atoms (Trp437 O−Trp453 NE1, 2.8 Å; Gln441 NE2−Ser445 OG, 2.7 Å; Gln441 OE1−Thr451 OG1, 2.8 Å). As in class D β-lactamases, this mobile loop is characterized by high-temperature factors, and in the BlaR-CTD crystal structure, the electron density around the Trp427−Glu436 region is relatively poor. By contrast, the BlaR-CTD Ω-loop (Ile474−Ser496), lying at the junction of the two domains, is stabilized by several H-bonds or hydrophobic interactions. As in all penicilloyl serine transferase structures, this loop delimits the bottom of the active site, and as in class D β-lactamase, a tryptophan residue (Trp488) points toward the catalytic cleft.

The loop connecting the β5 and β6 strands also seems to display a very high flexibility. In particular, residues Ile545 and Asn546 exhibit unclear electron densities, reflecting a disorder in the crystal. This β5−β6 loop also shows very high solvent-accessible surfaces for some hydrophobic residues. The accessible surface area computed throughout the BlaR-CTD structure, with the DSSP program (*18*), gives mean values of 38, 11, and 21 Å^2 for valine, isoleucine, and leucine residues, respectively. In comparison, Val544, Ile545, and Leu549 exhibit 3-fold higher or more accessible surfaces of 104, 70, and 73 Å^2, respectively. This loop, located at the C-terminal end of the β5 strand that delimits in part the active site, might be involved in some interactions specific to the biological function.

BlaR-CTD Active Site. The penicillin-binding site of BlaR-CTD is mainly delimited by four structural elements (Figure 3). The center of the catalytic pocket is occupied by the Ser402-Thr-Tyr-Lys405 tetrad that includes the nucleophilic serine residue at the amino-terminal end of helix α3. One side of the cavity is defined by the Ser450-Thr-Thr452 motif, connecting helices α4 and α5, while the opposite side is delimited by the Lys539-Thr-Gly541 triad lying on strand β5. The bottom is closed by the Ω-loop containing the Trp488 and Leu489 residues, which point into the active site. Of these four active site elements, the first three are relatively well conserved in all penicilloyl serine transferases characterized by the Ser*-Xaa-Xaa-Lys*, Ser(Tyr)-Xaa-Asn(Thr/Val), and Lys-Thr(Ser)-Gly* sequences, where the asterisk denotes a strictly conserved residue and the Xaa a variable one. The fourth element is more variable both in amino acid composition and in structural conformation. The Ω-loop most similar to that of BlaR-CTD is found in the class D β-lactamase structures with a tryptophan, equivalent to the BlaR-CTD Trp488, also followed by a hydrophobic residue (Ile or Leu). By contrast, the class A β-lactamase Ω-loop that bears the essential glutamate 166 residue acting as the general base in the catalytic process is totally different and very well conserved among this class of enzymes. In the class C β-lactamases, as well as in all known PBPs, this loop is once again different. The sole common characteristic for all of the different conformations of the loop observed in those two types of enzymes is a backbone carbonyl moiety always pointing toward the active site. This carbonyl group is that of the Ala220 residue in the class C β-lactamase from *Enterobacter cloacae* (*19*), of Ala237 in the DD-carboxypeptidase from *Streptomyces* R61 (*20*), of Asp143 in the DD-transpeptidase from *Streptomyces* K15 (*21*), and of Phe450, Tyr538, and Tyr450 in PBP2x from *Streptococcus pneumoniae* (*22*), PBP5 from *Enterococcus faecium* (*23*), and PBP2a from *S. aureus* (*24*), respectively.

Among the 81 water molecules defined in the BlaR-CTD crystal structure, mainly located in the first coordination shell, four are found in the active site, directly hydrogen bonded to the catalytic residues described above. The most conserved one, in all penicilloyl serine transferase structures, interacts with the oxyanion hole formed by the NH groups of Thr542, following the Lys539-Thr-Gly541 motif, and of the nucleophilic Ser402 residue.

Comparison with the Class D β-Lactamase Structures. All known 3D structures of class D β-lactamases, except that of the *E. coli* OXA-1 (PDB code 1M6K) (*25*), highlight a biologically active dimer with the two monomers related by

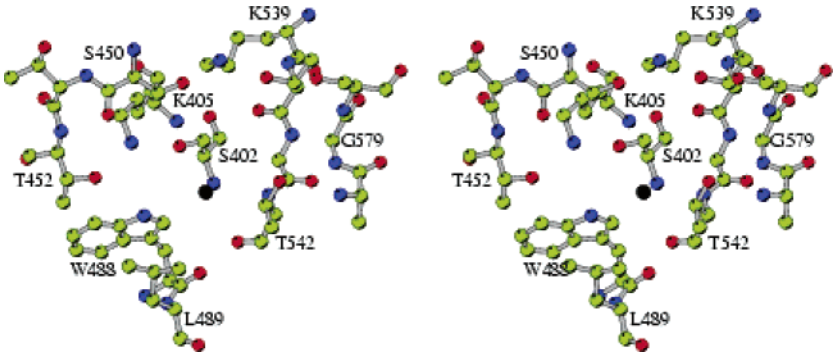

FIGURE 3: Stereoview of the active site of the BlaR-CTD domain with the three conserved motifs: the Ser402-Thr-Tyr-Lys405 tetrad, including the nucleophilic serine of motif 1, the Ser450-Thr-Thr452 motif 2, and the Lys539-Thr-Gly541 triad of motif 3. The bottom of the active site is defined by the Ω-loop bearing the Trp488 and Leu489 residues. The Gly579 residue equivalent to the conserved Arg250 of class D β-lactamases is also represented.

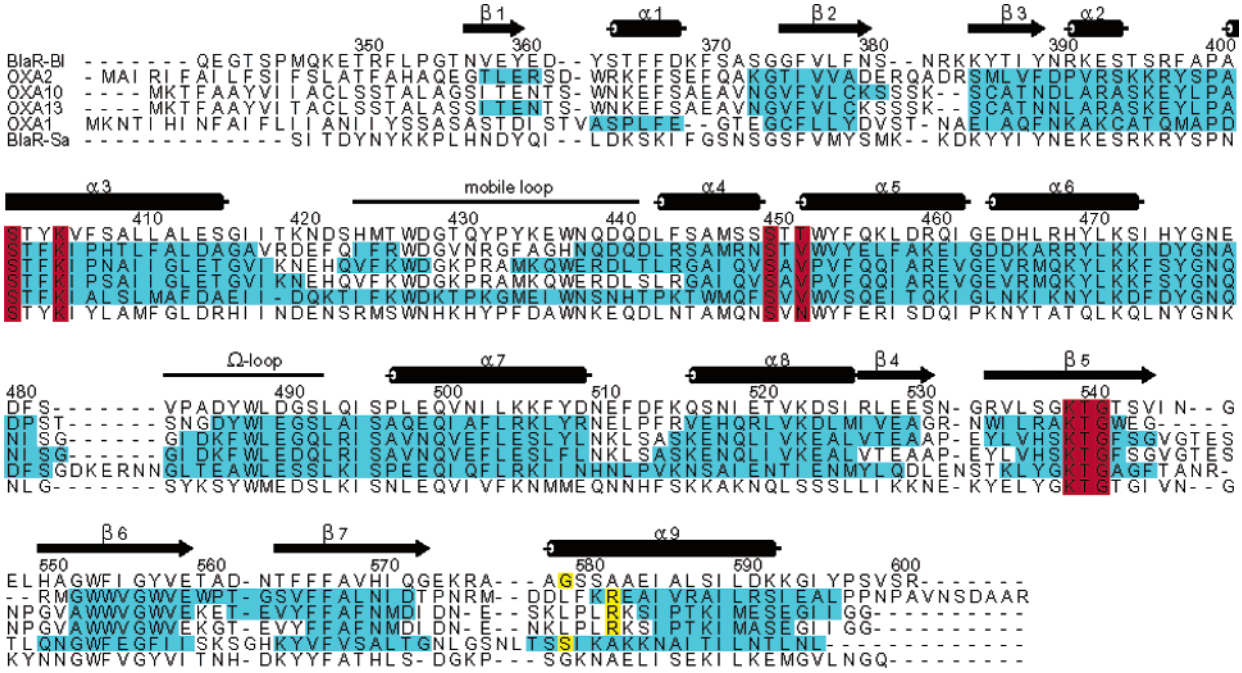

FIGURE 4: Amino acid sequence alignment of BlaR-CTD from *B. licheniformis* (BlaR-Bl) and from *S. aureus* (BlaR-Sa) and four class D β-lactamases, *S. typhimurium* OXA-2, *Ps. aeruginosa* OXA-10 and OXA-13, and *E. coli* OXA-1. The alignment is determined from 3D structure superposition, except for BlaR-Sa. The amino acid numbering and the secondary structures of BlaR-CTD are shown above the sequences. The three conserved active site motifs are in red, and the structurally superimposable regions between BlaR-CTD from *B. licheniformis* and each class D β-lactamase are in blue. The figure is produced with the program ALSCRIPT (*27*).

a 2-fold symmetry axis. The most significant elements for the dimerization are helix α8 and strand β4, with 2-fold symmetry-related residues lying on those secondary structures that are involved in various interactions such as hydrogen bond, hydrophobic cluster, and salt bridge formation. Several solvent molecules, water or ions, can also contribute to stabilize this quaternary architecture. As the BlaR-CTD crystallographic structure is composed of only one monomer, the comparison with class D β-lactamases will always refer to one monomer.

Superimpositions of the four class D β-lactamases OXA-2, OXA-10, OXA-1, and OXA-13 from *P. aeruginosa* (PDB code 1H8Z) (*26*) on BlaR-CTD were performed using the RIGID option of TURBO-FRODO. The fitting points were the equivalent Cα atoms of the catalytic residues Ser402, Lys405, Ser450, Thr452, Lys539, and Gly541. In each case, an initial distance cutoff of 1.0 Å was applied and progressively reduced to 0.2 Å. Considering only the backbone atoms (N, Cα, C, and O atoms) of structurally superimposable regions, the root mean square deviations of BlaR-CTD versus OXA-2, OXA-10, OXA-1, and OXA-13 are respectively 1.6, 1.9, 1.7, and 2.4 Å and correspond to 1138, 1149, 1126, and 1149 fitted atoms, respectively. On the basis of this X-ray structure superimposition, the amino acid sequence alignments reveal 32%, 24%, 25%, and 25% of strict identities, respectively (Figure 4). As already predicted by Zhu and co-workers (*4*), the penicillin-binding C-terminal domain of BlaR is quite similar to class D β-lactamases and particularly to OXA-2.

The most important differences between BlaR-CTD and the class D β-lactamases appear in the α1−β2 loop, the β5−β6 loop, and the β7−α9 loop with the N-terminal end of α9 (Figure 5A). These three regions are closely connected in the structure, and any modification of one of them certainly perturbs the others. However, the topology of the amino terminus of helix α9, lying along strand β5 delimiting the catalytic pocket, is quite similar in BlaR-CTD and OXA-1 when compared to the other class D enzymes. Indeed, the

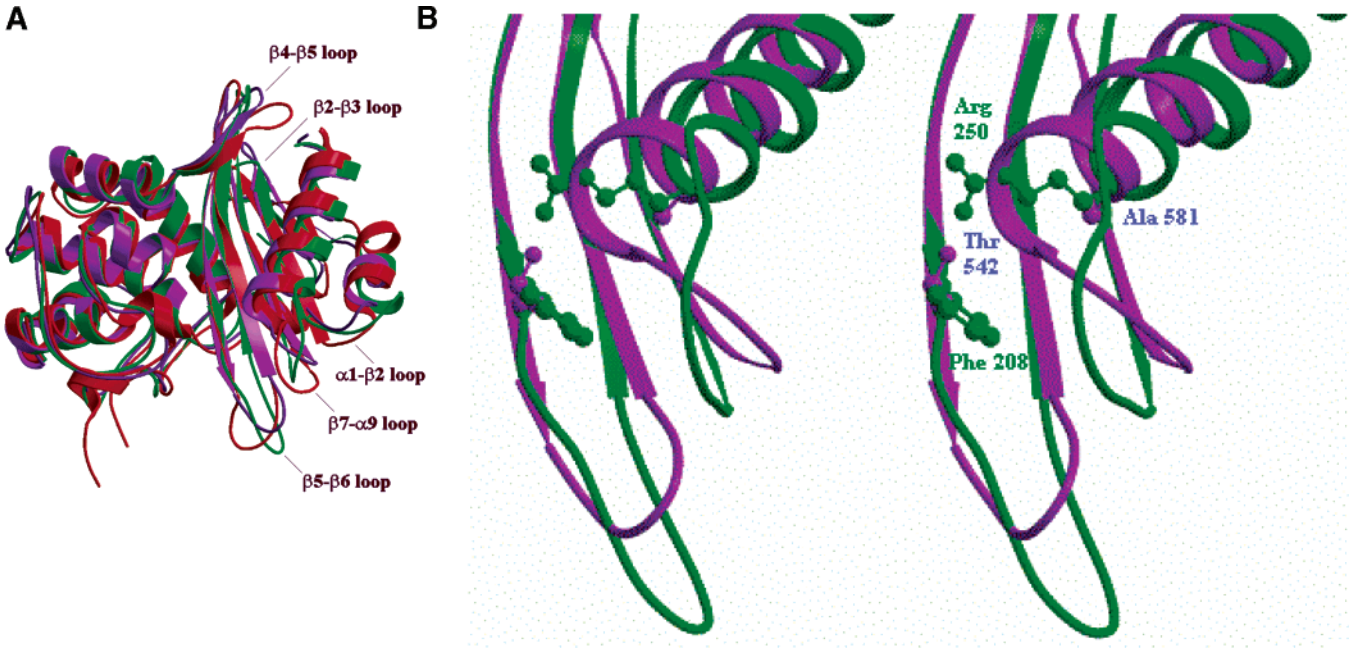

FIGURE 5: (A) Superimposed ribbon diagrams of BlaR-CTD (magenta) and of the class D β-lactamases OXA-10 (green) and OXA-1 (red). (B) Stereoview of the β5 strand and α9 helix regions of BlaR-CTD (magenta) and of the class D β-lactamase OXA-10 (green).

BlaR-CTD helix α9 begins one turn before the equivalent helix in OXA-2, OXA-10, and OXA-13, and for sterical reasons, this additional turn cannot tolerate a bulky side chain in position 542. This position, located just after the third catalytic motif Lys539-Thr-Gly541, is occupied by a phenylalanine in OXA-10 and OXA-13 or a tryptophan in OXA-2 and by a threonine and an alanine in BlaR-CTD and OXA-1, respectively (Figure 5B). Another feature incompatible with the BlaR-CTD α9 topology is the presence of a large side chain in position 582, an alanine in both BlaR-CTD and OXA-1. As already pointed out by Sun and co-workers (*25*), in the other subgroups of class D β-lactamases, the corresponding residue is an arginine that is directed to the active site. Equivalent to the class A β-lactamases Arg244 (or Arg220) (*28*), it makes electrostatic interactions with the carboxylate group of β-lactams, as observed in the structures of the moxalactam-OXA-10 (PDB code 1K6R) (*36*) and of the meropenem-OXA-13 (PDB code 1H8Y) (*26*) complexes. In BlaR-CTD, the position spatially equivalent to this arginine guanidinium group is residue Gly579 (Ser258 in OXA-1), which is strictly conserved, just like the Thr542 residue, in the sequences of BlaR from *S. aureus* and *Staphylococcus hemolyticus* and of MecR from *S. aureus*, *Staphylococcus epidermis*, and *Staphylococcus sciuri*.

Another region that also varies significantly is the β4−β5 loop. In BlaR-CTD, its conformation is intermediate between the one observed in OXA-1, which is a monomeric enzyme, and those observed in OXA-2, OXA-10, and OXA-13, which are dimers. Since this loop is involved in the class D dimerization process, its slight displacement in BlaR-CTD may be, at least in part, either responsible for its monomeric form or a result of this monomeric state. It is actually very difficult to determine which residues are necessary and/or sufficient for dimerization to occur, because the interactions involved at the dimerization surface are not specifically conserved among the class D structures.

The β2−β3 connecting loop is also variable, even in class D enzymes. Exposed to the solvent, the conformation of this region can be significantly influenced by the conformation of the N-terminal region. In vivo, as the N-terminal part of the penicillin-binding domain of the complete BlaR protein is anchored into the membrane, the constraints are certainly more important, reducing the flexibility of the N-terminal region and of its neighborhood. Some structural deviations are also found in the mobile loop, which is characterized by a relatively high conformational freedom. In the OXA-13 enzyme, this region is even more different, though not entirely defined in the crystal structure.

The relatively high rms deviation between the BlaR-CTD and OXA-13 structures is not solely due to the mobile loop but more generally to the whole α-domain which is relatively perturbed in OXA-13 when compared to OXA-2 and OXA-10. The reason is that, in those two latter structures, determined at pH 9.0 and 8.5, respectively, the lysine residue of the Ser67-Thr-Phe-Lys70 catalytic motif is carbonated, leading to a classical "active form" geometry of the catalytic cleft (Figure 6A). In the OXA-13 structure, determined at pH 5.5 (Figure 6B), Lys70 is not carbonated and adopts a conformation such that the second catalytic motif (Ser115-Ala-Val117) is entirely remodeled, leading to a large displacement of the mobile loop and perturbations in the α-domain (*26*). In BlaR-CTD, the electron density reveals unambiguously a "classical", not-carbonated, lysine residue in position 405 with its side chain pointing toward the catalytic pocket (Figure 7). This conformation is similar to that observed in all penicilloyl serine transferase structures, both in PBPs (Figure 6C) and in β-lactamases with the restriction described above for the class D β-lactamases.

To confirm that residue Lys405 of BlaR-CTD in its physiologically relevant form is not carbonated, the kinetic parameters (k_2/K) for the acylation of BlaR-CTD by cefalexin were determined in 50 mM phosphate buffer (pH 8, 50 mM NaCl) free of or supplemented with bicarbonate ion. The k_2/K values for degassed (CO_2-free) or not degassed samples were 1800 ± 270 $M^{-1}\cdot s^{-1}$ and 1540 ± 350 $M^{-1}\cdot s^{-1}$, respectively. Addition of 50 mM $NaHCO_3$ resulted in a

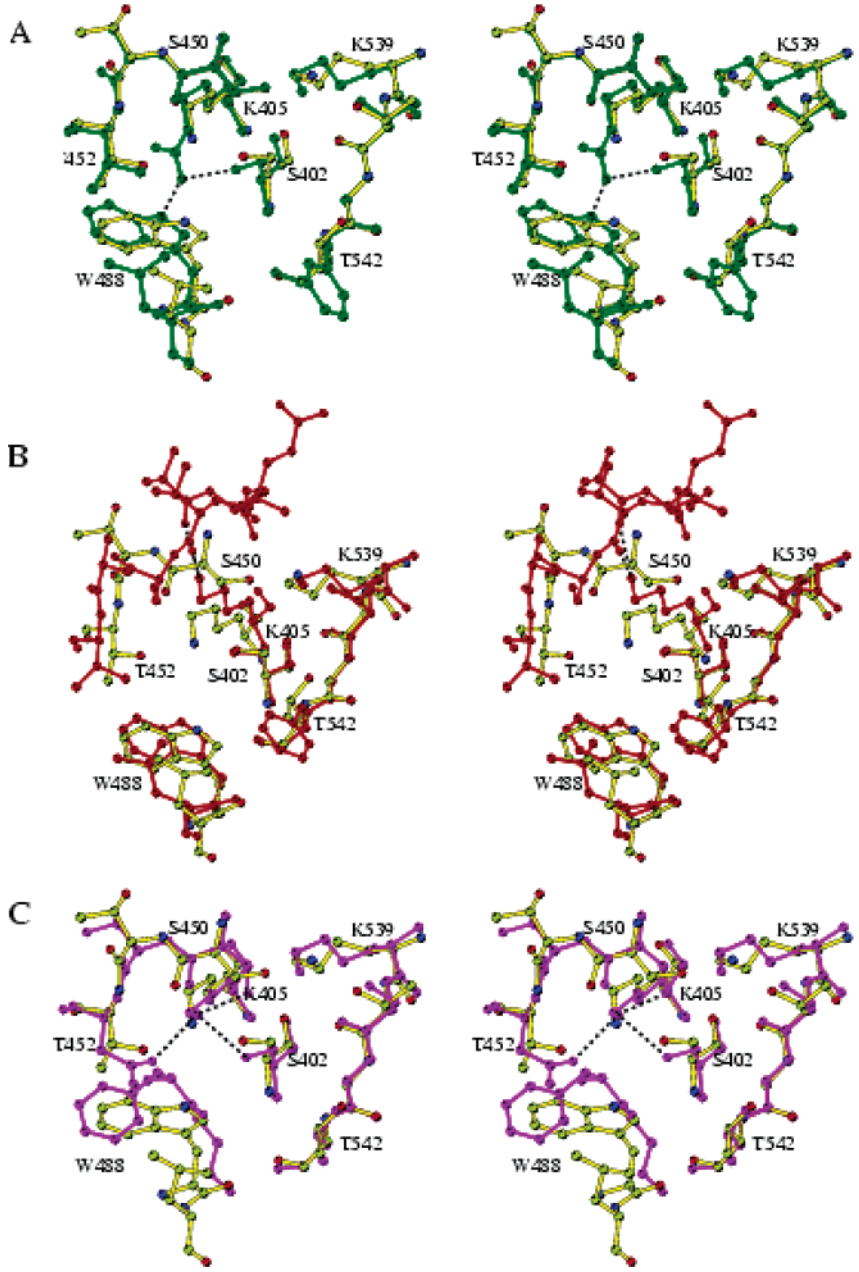

FIGURE 6: (A) Stereoview of the superimposed active sites of BlaR-CTD and of the class D β-lactamase OXA-10 (green). (B) Stereoview of the superimposed active sites of BlaR-CTD and of the class D β-lactamase OXA-13 (red). (C) Stereoview of the superimposed active sites of BlaR-CTD and of the penicillin-binding protein PBP2x from *S. pneumoniae* (magenta). Black dashed lines show the interactions of the lysine of the first conserved active site motif.

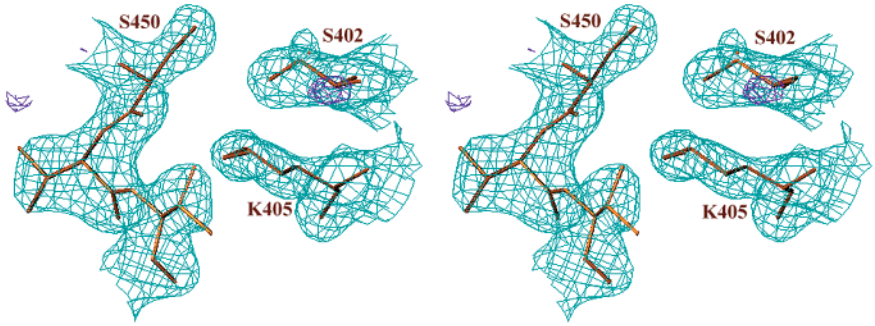

FIGURE 7: Stereoview of the electron density around the catalytic Lys405 residue. The $2F_o - F_c$ (cyan) and $F_o - F_c$ (blue) maps are contoured at 1.4σ and 2.5σ levels, respectively.

similar acylation rate of 1800 $\pm$ 270 $M^{-1}\cdot s^{-1}$. These values are similar to that obtained at pH 7.0 (*8*), 1700 $M^{-1}\cdot s^{-1}$. Those results clearly show that the kinetic parameters associated to BlaR-CTD are not modified by the presence

of bicarbonate or carbonate ions and, consequently, that the lysine of the first conserved motif is not modified in the BlaR-CTD active site.

DISCUSSION

BlaR-CTD Is a Highly Sensitive PBP. Even if the BlaR-CTD polypeptide chain adopts the class D β-lactamase folding and exhibits a similar active site topology, this sensor domain is a very sensitive PBP and not a β-lactamase. Indeed, previous kinetic studies of BlaR-CTD with various β-lactam antibiotics have revealed second-order acylation rate constants k_2/K' varying from 0.0017 $\mu M^{-1}\cdot s^{-1}$ to more than 1 $\mu M^{-1}\cdot s^{-1}$, with deacylation rate constants lower than 4×10^{-5} s^{-1}. These values reflect rapid formation of very stable acylated adducts (*8*). The most striking difference between the active sites of the penicillin-sensitive BlaR-CTD and of the class D β-lactamases is the state of the lysine residue defining the first catalytic motif Ser402-Xaa-Xaa-Lys405. In the class D β-lactamase 3D structures, the amino group of the corresponding lysine residue (Lys70) is surrounded by four almost strictly conserved hydrophobic side chains (Phe69, Val117, Trp154, and Leu/Ile155). This hydrophobic environment is believed to lower the Lys70 side chain pK_a, allowing its modification by carbonic anhydride. This carbonation is a pH-dependent phenomenon (*29*). At high pH values (greater than 8.5), all class D β-lactamase structures exhibit carbonated lysine in the first motif, and the catalytic pocket presents an "active conformation". At low pH values (below 5.5), this lysine is not carbonated, and the topology of the active site is perturbed. At the intermediate pH values, a mixture of the two states can be found. It is now commonly assumed that the carbonation of this lysine is essential to the class D enzyme catalytic activity, in both the acylation and deacylation steps. Here, we have shown that neither increasing the pH from 7.0 to 8.0 nor adding bicarbonate to the solution did significantly modify the rate of acylation by cefalexin.

According to these observations, the uncarbonated state of Lys405 observed in the BlaR-CTD structure, which has been solved at pH 6.95, could be due to the intermediate pH value. Under these conditions, and in contrast with the class D enzyme situation, the BlaR-CTD active site exhibits a classical active conformation (Figure 6A). This "classical active conformation" corresponds to a lysine side chain orientation in the active site equivalent to the one observed in the class A and C β-lactamases, and in PBPs, and also in class D β-lactamases but only when the corresponding lysine is carbonated. The conformation observed in BlaR-CTD can be explained by the lysine environment, a second important difference between BlaR-CTD and class D β-lactamases. Indeed, in the BlaR-CTD structure, the Lys405 side chain amino group interacts with the side chains of the active serine Ser402 and of Thr452, the third residue of the second active site motif. In all class D β-lactamases, this second motif always bears the Ser115-Xaa-Val117 signature. As pointed out above, the lysine environment is consequently much more hydrophobic, preventing the lysine 70 side chain from adopting the classical conformation and forcing it to rotate and create interactions with carbonyl groups of the polypeptide chain. These interactions with residues located just before the second motif induce another conformation of this polypeptide segment which orients the Ser115 side chain outside the active site. This situation is clearly incompatible with any enzymatic activity. On the other hand, when the lysine is carbonated, its longer side chain can be stabilized by an interaction with a conserved tryptophan lying on the bottom of the catalytic cleft. Under these conditions, the conformations of Lys70 and consequently of Ser115 are adequate for an efficient catalysis.

In brief, when compared to the class D β-lactamases, the substitution of a hydrophobic valine residue in the second motif by a polar residue such as threonine confers to BlaR-CTD an active site typical of all other penicilloyl serine transferases and, more precisely, of all other PBPs. Defined by the three conserved motifs Ser-Xaa-Xaa-Lys and Ser-Xaa-Asn(or Thr), the essential residues in the BlaR-CTD active site (Ser402, Lys405, and Ser450) are all in a conformation suitable for the acylation process. On the other hand, the protein is devoid of a residue acting as the general base required for the deacylation step and corresponding to glutamate 166 of the class A β-lactamases, the tyrosine 150 of the second motif in class C β-lactamases (*30*, *31*), or the carbamyl carboxylate of Lys70 in class D β-lactamases (*26*, *32*). One may note that the residue corresponding to Thr452 is always an asparagine in all other known BlaR and MecR sequences, as observed in most PBPs or in class A and C β-lactamases. Surprisingly, it was reported that the corresponding first catalytic motif lysine residue in the BlaR-CTD from *S. aureus* (Lys392) is carbonated (*9*). The difference of behavior between the two BlaR-CTDs remains obscure to us. Indeed, on the basis of their amino acid sequence alignment (Figure 4), one may postulate that the two penicillin sensor 3D structures are similar and that the Lys392 environment is the same as the one described in the active site of the BlaR-CTD from *B. licheniformis*. Only the knowledge of the 3D structure of the BlaR-CTD from *S. aureus* would shed light on the catalytic mechanism difference between both penicillin sensors.

Another feature of the PBP active site is the polar character of the residue following the third conserved motif Lys-Thr-Gly, generally a threonine (*25*). This residue in BlaR-CTD is Thr542, and it is conserved in the sequences of BlaR from *S. aureus* and *S. hemolyticus* and of MecR from *S. aureus*, *S. epidermis*, and *S. sciuri*. In the class D β-lactamases, the corresponding residue is often large and hydrophobic (Trp or Phe), except in the OXA-1 subgroup, but in that case the hydrophobic characteristic can be supplied by residues in the $\beta7-\alpha9$ loop (Leu255 in OXA-1, position 576 in Figure 4). Both substitutions, Val to Thr452 and Trp/Phe to Thr542, modify the hydrophobic and electrostatic properties of the class D enzyme catalytic pocket when compared to BlaR-CTD and certainly affect the substrate affinity and activity profiles. Thus, it is not surprising that BlaR-CTD recognizes benzylpenicillin better than cloxacillin (*8*), as do many PBPs and in contrast with the class D β-lactamases (*29*, *33*).

Transmembrane Induction Mechanism. Many signal-transducing receptors are membrane-bound proteins with an extracellular domain, the sensor that recognizes specific inducer molecules, such as hormones, growth factors, or neurotransmitters. The interaction between the inducer and the sensor generates a signal transmitted through the membrane eliciting a response of the intracellular domain. The response often activates cascades of enzymatic reactions, resulting in many different effects within the cell (*34*). Here,

the first step of the β-lactamase induction process, the signal transmission from the outer to the inner of cell, is discussed. The sensor is BlaR-CTD, the inducers are β-lactam antibiotics, and the transmission is mediated by the four transmembrane segments TM1 to TM4 (Figure 1), which have been predicted to form a four-α-helix bundle (*2*). The relative positions of these four segments in the membrane are conditioned by the loops that interconnect them. Conversely, any modification of the orientation of those segments must, via their N- and C-terminal ends, influence the folding of the BlaR intracellular and extracellular loops or domains. Any modification of the relative orientations of the transmembrane segments, at least of TM3 and/or TM4, would result in the transmission of a signal from the cell outer surface to the intracellular loop L3.

Without the BlaR-CTD domain, there is no β-lactamase induction, indicating that the relative positions of the four transmembrane segments are inefficient to induce the hydrolytic activity of the loop L3. On the other hand, in *S. aureus*, a truncated version of BlaR where 6 amino acids substitute for the 35 C-terminal residues confers constitutive synthesis of β-lactamase (*35*). Since the amino acid sequences of the BlaR proteins from *B. licheniformis* and *S. aureus* are similar, the BlaR truncated form would correspond to a BlaR-CTD protein devoid of the β7−α9 loop, of helix α9, and of the C-terminal region. The interactions of the transmembrane region with the truncated BlaR-CTD are thus similar to those of the native BlaR-CTD after acylation by a β-lactam. These two observations show that BlaR-CTD naturally imposes constraints onto the extracellular domains and by extension to the transmembrane regions. Modifications of these constraints are necessary to the signal transmission and occur when BlaR-CTD binds a β-lactam or when its C-terminal region is removed.

It is presently not possible yet to decide which BlaR-CTD regions or residues are directly involved in the interaction scheme with the other extracellular elements. The deciphering of the transmembrane induction mechanism details remains to be clarified by further analysis of complex structures. Useful 3D structures would be these of the BlaR-CTD acylated by a β-lactam or in interaction with the extracellular L2 loop and of the whole membrane BlaR protein.

ACKNOWLEDGMENT

We are grateful to the BM30A/FIP beamline's staff at ESRF for assistance. We thank M. Vermeire for expert assistance with data collection and D. Engher for work in early protein crystallization.

REFERENCES

1. Joris, B., Hardt, K., and Ghuysen, J. M. (1994) pp 505−515, Elsevier, Amsterdam, London, New York, and Tokyo.
2. Hardt, K., Joris, B., Lepage, S., Brasseur, R., Lampen, J. O., Frère, J.-M., Fink, A. L., and Ghuysen, J.-M. (1997) *Mol. Microbiol. 23*, 935−944.
3. Zhang, H. Z., Hackbarth, C. J., Chansky, K. M., and Chambers, H. F. (2001) *Science 291*, 1962−1965.
4. Zhu, Y., Englebert, S., Joris, B., Ghuysen, J.-M., Kobayashi, T., and Lampen, J. O. (1992) *J. Bacteriol. 174*, 6171−6178.
5. Sherratt, D. J., and Collins, J. F. (1973) *J. Gen. Microbiol. 76*, 217−230.
6. Filée, P., Benlafya, K., Delmarcelle, M., Moutzourelis, G., Frère, J. M., and Joris, B. (2001) *Mol. Microbiol. 44*, 685−694.
7. Joris, B., Ledent, P., Kobayashi, T., Lampen, J. O., and Ghuysen, J. M. (1990) *FEMS Microbiol. Lett. 58*, 107−113.
8. Duval, V., Swinnen, M., Lepage, S., Brans, A., Granier, B., Franssen, C., Frère, J.-M., and Joris, B. (2003) *Mol. Microbiol. 48*, 1553−1564.
9. Golemi-Kotra, D., Cha, J. Y., Meroueh, S. O., Vakulenko, S. B., and Mobashery, S. (2003) *J. Biol. Chem. 278*, 18419−18425.
10. Jancarik, J., and Kim, S.-H. (1991) *J. Appl. Crystallogr. 24*, 409−411.
11. McPherson, A. (1999) *Crystallization of Biological Macromolecules*, Cold Spring Harbor Laboratory Press, Cold Spring Harbor, NY.
12. Leslie, A. G. R. W. (1996) MOSFLM Version 5.40, Mosflm Users Guide.
13. CCP4, Number 4 (1994) *Acta Crystallogr. D50*, 760−763.
14. Navaza, J. (1994) *Acta Crystallogr. A50*, 157−163.
15. Roussel, A., and Cambillau, C. (1989) *Silicon Graphics Geometry Partner Directory*, pp 77−78, Silicon Graphics, Mountain View, CA.
16. Brünger, A. T., Adams, P. D., Clove, G. M., Delano, W. L., Gros, P., Grosse-Kunsteve, R. W., Jiang, J.-S., Kuszewski, J., Nilges, M., Pannu, N. S., et al. (1998) *Acta Crystallogr. D54*, 905−921.
17. Kraulis, P. J. (1991) *J. Appl. Crystallogr. 24*, 946−950.
18. Kabsch, W., and Sander, C. (1983) *Biopolymers 22*, 2577−2637.
19. Lobkovsky, E., Moews, P. C., Liu, H., Zhao, H., Frère, J.-M., and Knox, J. R. (1993) *Proc. Natl. Acad. Sci. U.S.A. 90*, 11257−11261.
20. Kelly, J. A., Knox, J. R., Zhao, H., Frère, J.-M., and Ghuysen, J.-M. (1989) *J. Mol. Biol. 209*, 281−295.
21. Fonzé, E., Vermeire, M., Nguyen-Distèche, M., Brasseur, R., and Charlier, P. (1999) *J. Biol. Chem. 31*, 21853−21860.
22. Gordon, E., Mouz, N., Duée., E., and Dideberg, O. (2000) *J. Mol. Biol. 299*, 477−485.
23. Sauvage, E., Kerff, F., Fonzé, E., Herman, R., Schoot, B., Marquette, J.-P., Taburet, Y., Prevost, D., Dumas, J., Leonard, G., Stefanic, P., Coyette, J., and Charlier, P. (2002) *Cell. Mol. Life Sci. 59*, 1223−1232.
24. Lim, D., and Strynadka, N. C. J. (2002) *Nat. Struct. Biol. 9*, 870−876.
25. Sun, T., Nukaga, M., Mayama, K., Braswell, E. H., and Knox, J. (2003) *Protein Sci. 12*, 82−91.
26. Pernot, L., Frénois, F., Rybkine, T., L'Hermite, G., Petrella, S., Delettré, J., Jarlier, V., Collatz, E., and Sougakoff, W. (2001) *J. Mol. Biol. 310*, 859−874.
27. Barton, G. J. (1993) *Protein Eng. 6*, 37−40.
28. Jacob, F., Lamotte-Brasseur, J., Dideberg, O., Joris, B., and Frère, J.-M. (1991) *Protein Eng. 4*, 811−819.
29. Golemi, D., Maveyraud, L., Vakulenko, S., Samama, J.-P., and Mobashery, S. (2001) *Proc. Natl. Acad. Sci. U.S.A. 98*, 14280−14285.
30. Jamin, M., Wilkin, J. M., and Frère, J.-M. (1995) *Essays Biochem. 29*, 1−24.
31. Knox, J. R., Moews, P. C., and Frère, J.-M. (1996) *Chem. Biol. 3*, 937−947.
32. Maveyraud, L., Golemi, D., Kotra, L. P., Tranier, S., Vakulenko, S., Mobashery, S., and Samama, J.-P. (2000) *Struct. Folding Des. 8*, 1289−1298.
33. Ledent, P., Raquet, X., Joris, B., Van Beeumen, J., and Frère, J.-M. (1993) *Biochem. J. 292*, 555−562.
34. Branden, C., and Tooze, J. (1999) *Introduction to Protein Structure*, 2nd ed., Garland Publishing, New York.
35. Lewis, R. A., Curnock, S. P., and Dyke, K. G. H. (1999) *FEMS Microbiol. Lett. 178*, 271−275.
36. Kerff, F. (2002) Ph.D. Thesis, University of Liège, Belgium.

BI034976A